NMR instabilities and spectral clustering in laser-polarized liquid xenon

K. L. Sauer,* F. Marion, P. J. Nacher, and G. Tastevin
Laboratoire Kastler Brossel, Ecole Normale Supérieure, 24 rue Lhomond, F75005 Paris, France
(Received 1 September 2000; published 20 April 2001)

To study how highly magnetized liquids behave in NMR experiments, we have performed low-field NMR on laser-polarized liquid ^{129}Xe, with nuclear polarization of up to 6%. Contrary to conventional NMR results, we find that instabilities develop after a large pulse, leading to an unexpectedly abrupt decay of the signal. In contrast, the NMR spectrum after a small pulse collapses to a series of unusually sharp lines (spectral clustering), whose widths correspond to precession lifetimes longer than a half minute. We discuss the key role of long-range dipolar coupling in such spin dynamics.

DOI: 10.1103/PhysRevB.63.184427 PACS number(s): 76.60.Jx

In conventional NMR the dipolar field created by the magnetization of the sample is small and usually has a negligible effect compared to that of the external fields. However, for a highly magnetized sample, as found in high-resolution NMR or in low-temperature physics, it can lead to unusual dynamical and spectral NMR behavior. Multiple spin echoes,[1] modulated NMR absorption spectra,[2] and tip-angle-dependent precession lifetimes[3,4] have been observed in thermally polarized liquid or solid ^{3}He. Liquefaction of laser-polarized noble gases introduces a new class of dense samples with very high and field-independent magnetization. With low-field NMR, spin dynamics can be probed in a regime where the dipolar field dominates the external field variations over the sample.

Using optical pumping techniques, Nacher *et al.*[5–7] prepared U-shaped samples of liquid ^{3}He and ^{3}He-^{4}He mixtures with large nonequilibrium polarizations. At small tip angles they observed sets of very sharp lines instead of a continuous spectrum (spectral clustering), corresponding to long-lived spatial distributions of phase-locked transverse magnetization (magnetization modes) precessing at distinct eigenfrequencies.[8,9] Response to larger tip angles died out much more rapidly, suggesting the existence of instabilities.[10] The genuine origin of these effects lies in the complex combination of long-range dipolar interactions. In a recent theoretical study Jeener suggests that spectral clustering, as well as instabilities obtained at large tip angles, are generic features of dipolar field effects in highly magnetized samples.[11]

In this paper we describe a systematic study of NMR free-induction decays (FID) in optically polarized liquid ^{129}Xe. Observation of spectral clustering and instabilities demonstrates the truly classical nature of these phenomena. Quantitative investigation of decay rates provides clues about the dynamical robustness of magnetization modes and the onset of turbulent spin motion at large tip angles.

The contribution to the Bloch equation for the magnetization $\boldsymbol{\mathcal{M}}$ at a point $\mathbf{r}$ due to the dipolar field created by the remainder of the sample can be written as

$$\frac{\partial \boldsymbol{\mathcal{M}}(\mathbf{r})}{\partial t} = \frac{\gamma \mu_0}{8\pi} \int d^3\mathbf{r}' \frac{(3\cos^2\theta - 1)}{|\mathbf{r}' - \mathbf{r}|^3} \boldsymbol{\mathcal{M}}(\mathbf{r}) \times [2\mathcal{M}_z(\mathbf{r}')\hat{\mathbf{z}} - \boldsymbol{\mathcal{M}}_\perp(\mathbf{r}')],$$

where the angular dependence of the integrand results from a straightforward secular approximation in the rotating Larmor frame (θ is the angle between $\mathbf{r}' - \mathbf{r}$ and static field axis $\hat{\mathbf{z}}$; γ is the gyromagnetic ratio). Computing the dynamical evolution of $\boldsymbol{\mathcal{M}}$ from this contribution is generally a formidable task. If one assumes the direction of $\boldsymbol{\mathcal{M}}_\perp$ to be uniform, $\mathcal{M}_z$ simply remains unchanged and a shift from Larmor precession is induced for $\boldsymbol{\mathcal{M}}_\perp$. In an anisotropic sample, even with uniform $\mathcal{M}_z$, the angular factor does not integrate out and a point-dependent shift can result. One may yet find distributions of the amplitude of $\boldsymbol{\mathcal{M}}_\perp$ that can exactly compensate for the spatial variations of the angular factor, providing stationary solutions for the Bloch equation with uniform (and shifted) frequencies. Such eigenmodes correspond to the observed magnetization modes and have been quantitatively determined using a model with a one-dimensional (1D) approximation of the dipolar couplings.[8,12] In contrast, spatial variations of the direction of $\boldsymbol{\mathcal{M}}_\perp$ give rise to changes in $\mathcal{M}_z$ and the nonlinear coupling between $\mathcal{M}_z$ and $\boldsymbol{\mathcal{M}}_\perp$ comes into play. The stability of the magnetization modes against small perturbations is not known yet. Using numerical simulations and analytical calculations Jeener found threshold values for tip angles above which instabilities may develop.[11]

To have a well-defined geometry and facilitate comparison with work in liquid He,[6–9] we use a U-shaped tube to contain the liquid Xe. As shown in Fig. 1, our experimental glass cell consists of a 12-mm-inner-diameter spherical optical pumping volume (OPV) connected to a U tube of inner diameter 0.6 mm. We sealed 180 μmol of 99.9%-enriched ^{129}Xe, 6 μmol of N_2 gas, and a few milligrams of Rb within the cell. The cell is internally coated with dimethyldichlorosilane to reduce nuclear relaxation.

The production of polarized liquid Xe is performed in two steps: ^{129}Xe is polarized as a gas in the OPV and then condensed into the U tube. In the first step, the Rb D_1 line is optically pumped with circularly polarized light from a 2-nm-broad 40-W diode laser bar. N_2 here serves as a quenching gas. The Rb polarization is transferred to the ^{129}Xe nucleus by spin exchange.[13–15] The OPV is kept at a temperature of about 350 K while the bottom of the U is maintained above 190 K to ensure that no Xe is condensed and most of it lies in the OPV. A ^{129}Xe polarization of 10%

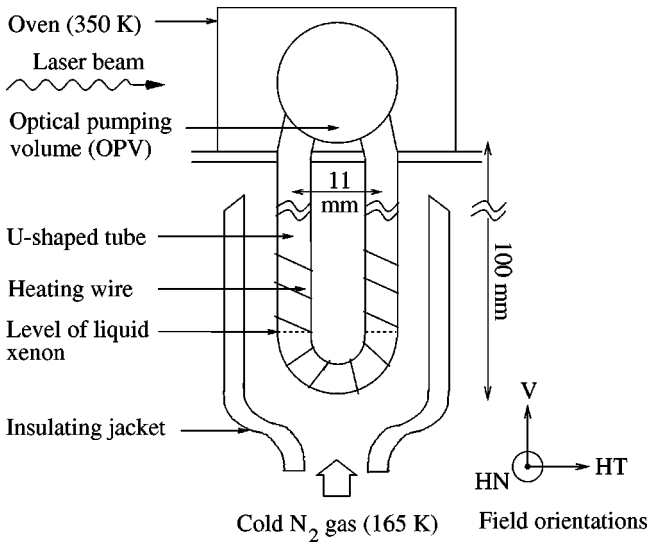

FIG. 1. Experimental setup. Temperature control of the OPV uses a hot air flow, that of the U a cold gaseous nitrogen flow. During optical pumping, a heating wire prevents Xe from condensing in the U. Afterwards, it is turned off and the polarized ^{129}Xe liquefies to fill the bottom of the U.

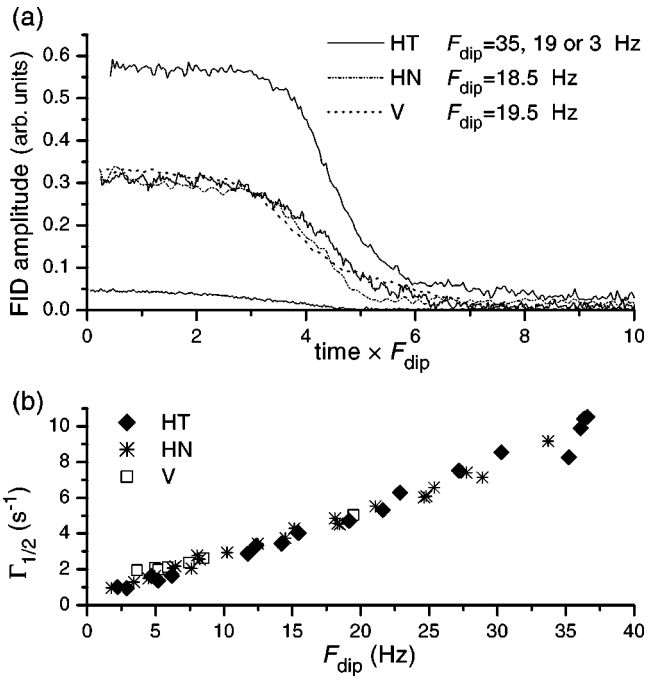

FIG. 2. (a) FID signal amplitudes for a 90° tip angle are plotted as a function of a reduced time. The dipolar frequency F_{dip} is proportional to the initial magnetization density (see text). (b) Signal decay rates are plotted as a function of F_{dip} for three different field directions (HT, HN, and V, see Fig. 1).

can be reached in 30 min. When optical pumping is complete, the bottom part is cooled to 165 ± 1 K. After a few minutes the system is thermally stable and two thirds of the Xe is liquefied, filling 5 mm^3 inside the U (up to the ''arms,'' see Fig. 1). In the liquid the relaxation time is $T_1 = 20$ min and the highest polarization obtained is 6%.

Pulsed NMR is performed in a magnetic field $B = 1.7$ mT (Larmor frequency $F_{Lar}=20$ kHz for ^{129}Xe) with three possible directions for the field, defined with respect to the cell (V: vertical, HT: horizontal tangent, and HN: horizontal normal, see Fig. 1). Optical pumping is performed with B along HT, and the gas magnetization is monitored in the OPV using a cross-coil NMR probe. To study the liquid, different sets of NMR probes are used for a vertical and a horizontal B. Magnetization follows adiabatically the direction of B as the field is switched from horizontal to vertical.

The field homogeneity over the sample is shimmed using additional gradient coils, leading to precession half-life times $T^*_{2\,inh}\simeq 1$ s as measured at 300 K in a 1-cm spherical cell filled with 3 bars of Xe gas (with negligible dipolar effects). As a measure of the magnitude of the dipolar field in the liquid ^{129}Xe, we introduce the *dipolar frequency* $F_{dip} = (\gamma/2\pi)\mu_0\mathcal{M}$, from the magnetization $\mathcal{M}=\mu_n NP$ (μ_n is the magnetic moment of the ^{129}Xe nucleus, N the ^{129}Xe number density, and P the polarization). In our experiment $F_{dip}=0.8\times P$ kHz and the dipolar field is larger than the field inhomogeneities over the sample even for P as low as 1%.

Magnetization is tipped using a resonant rf field B_1 at F_{Lar} such that dipolar effects during the pulse are negligible ($\gamma B_1 \gg 2\pi F_{dip}$). F_{dip} (and hence P) are deduced from the analysis of FID signals (see below). Because the observed signals are often nonexponential, we choose to characterize each decay by the rate $\Gamma_{1/2}$, defined as the inverse of the FID half-life time.

FID signals recorded after 90° tipping pulses have been studied as a function of field direction and initial dipolar frequency. Lifetimes range from 1–2 s for low F_{dip} to 0.1 s for higher F_{dip}. A reduced time (time multiplied by F_{dip}) is thus used to conveniently compare the time variations of the FID signals, which all present similar features [see Fig. 2(a)]. Precession occurs at F_{Lar}. Amplitude is almost constant during the first part of the precession (approximately 4 periods of F_{dip}). Then the signal decreases abruptly, this decrease being more abrupt for larger F_{dip}. Decay rates increase fairly linearly with F_{dip} [see Fig. 2(b)], which justifies using F_{dip} to define a reduced time. Time evolutions are independent of the direction of B.

For small tip angles, behaviors are qualitatively different and depend much on the field direction. Figure 3(a) shows spectra computed by fast Fourier transform (FFT) of FID signals recorded in a vertical B for various F_{dip}. All spectra present two sets of lines, one on each side of F_{Lar}, with shifts from F_{Lar} scaling with F_{dip}. Applying known field gradients, we could attribute the lines on the left (the less shifted) to the magnetization precession in the U bottom, and the lines on the right to the precession in the U arms. Linewidths change dramatically with polarization. They increase with F_{dip}, the lines associated with the U arms remaining the broadest. At low F_{dip} the lines associated with the U bottom are very narrow and well resolved. They form structures that are quite similar to those of Refs. 6–8 obtained

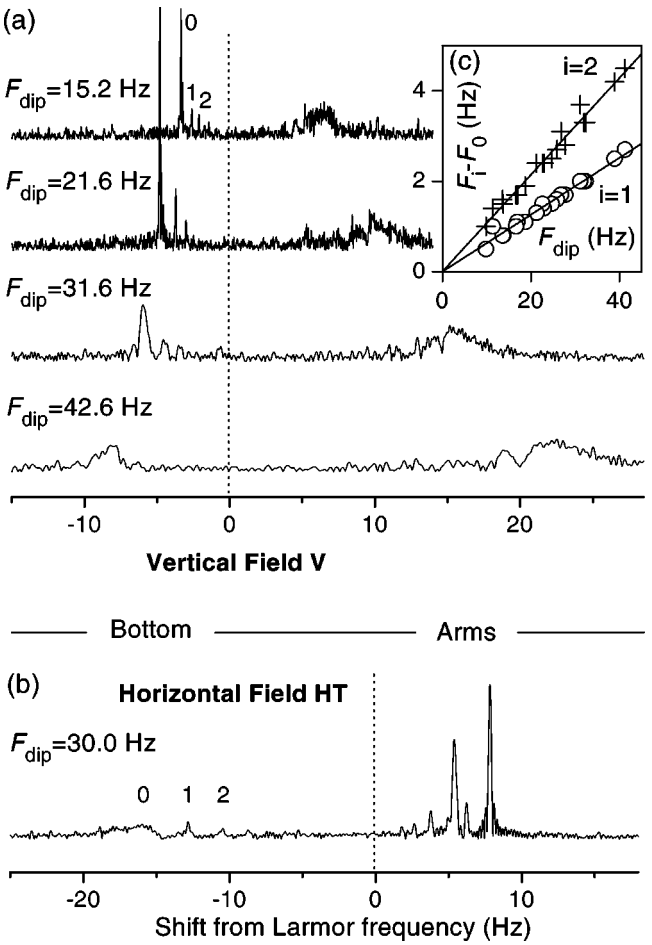

FIG. 3. NMR spectra after a 7.9° tip angle for (a) different magnetization densities in a vertical field and (b) one in a HT-horizontal field. The main modes in the U bottom are labeled 0, 1, and 2. In (b) a small gradient has been applied along HT to shift Larmor frequencies by ± 2 Hz in the U arms and clearly separate the corresponding sets of modes. In (c) frequency splittings with respect to mode 0 in a vertical field are compared to computed expectations [solid lines (Ref. 12)].

with He mixtures (magnetization modes for a vertical U in a vertical field). Given our system dimensions, using F_{dip} as the only fitting parameter, the positions of all observed and computed lines[8,12] can be accurately matched [Fig. 3(c)]. This determination of F_{dip} is consistent with an estimation of P from the signal amplitude.

Experiments have been repeated with B along HT. One typical spectrum is plotted in Fig. 3(b). For figure clarity, it has been recorded with the opposite polarization, so that the lines on the left (now the most shifted from F_{Lar}) still correspond to the magnetization modes in the bottom. In contrast with the vertical field situation, the modes in the arms are now long lived, whereas modes in the bottom are short lived. The stability of a mode is thus found to depend on the orientation of the local curvature of the cell with respect to B, rather than on shape or boundary effects in the arms.

With B along HN, all elements of the sample can be expected to experience the same dipolar shift. This configuration has been briefly studied. Indeed all NMR spectra have been observed to be shifted from F_{Lar} by about $-F_{dip}/4$ and to extend over at most 1 Hz. We obtained, however, sets of narrow lines for small tip angles that need to be further investigated.

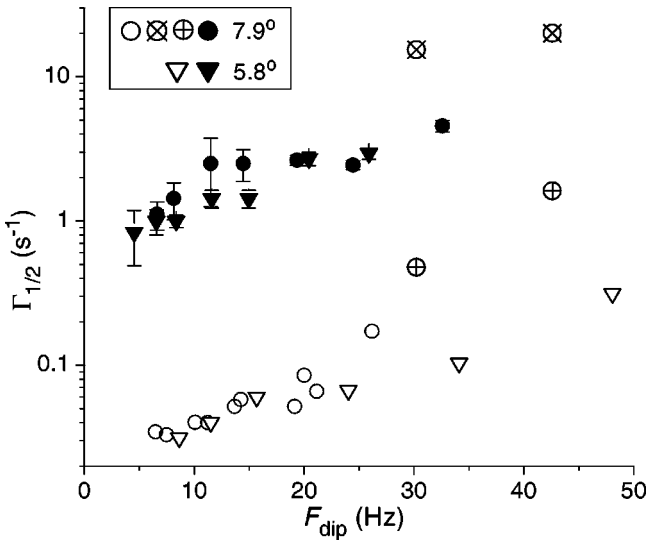

FIG. 4. Decay rates of mode 0 localized in the U bottom in a vertical field (open symbols) and a HT-horizontal field (filled symbols) for two values of the tip angle. The crossed open symbols correspond to nonexponential decays (see text).

Figure 3(a) shows that for a vertical B the modes in the bottom (0,1,2. . .) become more stable when F_{dip} decreases. Using inverse FFT of band-pass filtered spectra, the time evolution of mode 0 has been tracked and quantitatively studied, both for B along V and along HT. The resulting $\Gamma_{1/2}$ are plotted for two different tip angles as a function of F_{dip} in Fig. 4. For a vertical B two decay regimes can be observed. The first regime occurs at low polarization or a very small tip angle. For tip angles up to the largest studied (15°), exponential decays with very long (up to 40 s) angle-independent lifetimes have been observed for sufficiently low polarization. For tip angles below (7°), this regime was observed over the whole polarization range studied. Decays that could be characterized by a single exponential are plotted as open symbols in Fig. 4. The second regime was observed for angles larger than (7°) at high polarization. The decays are nonexponential and present a complex structure with a clear two-step decrease from which two half-life times are unambiguously extracted (plotted as crossed symbols in Fig. 4). Finally, with B along HT nonexponential decays are always obtained, characterized by a single fast decay rate (filled symbols in Fig. 4).

To conclude, spectral clustering is consistently observed for small tip angles. The line positions are successfully described by the model previously used for NMR in liquid He.[8,12] This consistency strongly supports the model's basic assumption, namely, that spectral clustering arises from classical dipolar coupling over macroscopic dimensions and does not involve the quantum properties of low-temperature He fluids.

The decay rates of FID signals have been systematically studied by varying the tip angle, the field direction, and the

polarization. We have checked that they are not related to the processes that usually control decay rates in conventional NMR. First, decay rates in this experiment do not significantly depend on applied gradients (in contrast with $1/T^*_{2\,inh}$ for a system with negligible F_{dip}). $\Gamma_{1/2}$ much shorter or longer than $1/T^*_{2\,inh}$ have been recorded [Fig. 2(b); Fig. 4]. Second, the contribution of radiation damping effects has been estimated to reach at most a few 10^{-2} s^{-1}. Consistently, no significant dependence on the sign of $\mathcal{M}_z$ was observed for long-lived signals. Radiation damping is thus believed to have a negligible effect for fast decays at large tip angles.

The abrupt signal decays we observe at high F_{dip} and large tip angles may be related to the onset of turbulent spin motion and the strong decrease in total magnetization obtained in numerical simulations.[11] Jeener also computed the exponential growth rate of deviations from uniform $\boldsymbol{\mathcal{M}}$ in the bulk of an isotropic magnetized sample and found it to be proportional to F_{dip}.[11] For 90° pulses, decay rates experimentally scale with F_{dip} and strikingly enough, do not depend on the field direction with respect to our anisotropic sample. However, fits of the departures from initial FID amplitudes give exponential growth rates three to ten times smaller than Jeener's (7.2 s^{-1} at $F_{dip}=2.4$ Hz for negligible diffusion), depending on F_{dip}. Sample edge effects and long-term evolution of the magnetization still have to be included in the calculations to allow quantitative comparison and fully describe the observations.

Instabilities are observed to occur in liquid Xe (see Fig. 4) at a much smaller tip angle than predicted in Ref. 11 (above 35°). This confirms recent results obtained in laser-polarized He.[10,16] Below the onset of instabilities, long-lived magnetization modes result in the observed spectral clustering. These spatially nonuniform modes should be damped by spin diffusion. Using the 1D model of Refs. 8 and 12, the computed decay rate of the most-shifted mode in the U bottom [mode 0 in Fig. 3(a)] is $\Gamma^{diff}_{1/2}=0.18\times10^{-2}$ s^{-1}, independent of tip angle and of F_{dip}. This does not account for the observed $\Gamma_{1/2}$ (Fig. 4), and the origin of these F_{dip}-dependent decay rates is unclear. Spin diffusion does, however, put a lower limit on the observable decay rates. The very long mode lifetimes measured for liquid Xe thus could not have been obtained in liquid ^{3}He-^{4}He mixtures, which have much larger spin-diffusion coefficients. Yet they form a consistent extension to the He data, which correspond to higher F_{dip} (100–600 Hz) in a similar geometry.[8,16] Our Xe experiment shows that the decay rates in this small angle regime strongly depend on the sample-field orientation. This unanticipated result needs further investigation and explanation.

From our results, a substantial body of data can be extracted that puts severe constraints on models developed to account for NMR observations in highly magnetized samples. Quantitative discrepancies with existing predictions and unanticipated new features call for an improved comprehensive description of the nuclear-spin dynamics. Investigations for different sample shapes are in progress in laser-polarized liquids.[16] Dipolar field effects similar to those presented in this paper are expected to be observed in conventional high-resolution NMR experiments in liquids, as soon as relaxation and radiation-damping processes get under efficient control in high-field spectrometers.[11,17]

We thank Jean Jeener for stimulating discussions and for communicating unpublished results. We gratefully acknowledge support from the French Ministry of Foreign Affairs and the Dephy Association (for K.S.).

*Present address: Code 6122, Chemistry Division, Naval Research Laboratory, Washington, D.C. 20375.

[1] G. Deville, M. Bernier, and J.M. Delrieux, Phys. Rev. B **19**, 5666 (1979).
[2] D.D. Osheroff and M.C. Cross, Phys. Rev. Lett. **59**, 94 (1987).
[3] J.R. Owers-Bradley, O. Buu, C.J. McGloin, R.M. Bowley, and R. Konig, Physica B **284**, 190 (2000).
[4] T. Matsushita, R. Nomura, H.H. Hensley, H. Shiga, and T. Mizusaki, J. Low Temp. Phys. **105**, 67 (1996).
[5] G. Tastevin, P.J. Nacher, L. Wiesenfeld, M. Leduc, and F. Laloe, J. Phys. (France) **49**, 1 (1988).
[6] P.J. Nacher, D. Candela, and M.E. Hayden, Physica B **194**, 847 (1994).
[7] D. Candela, M.E. Hayden, and P.J. Nacher, Phys. Rev. Lett. **73**, 2587 (1994).
[8] P.J. Nacher, E. Stoltz, and G. Tastevin, Czech. J. Phys. **46**, 3025 (1996).
[9] P.J. Nacher and E. Stoltz, J. Low Temp. Phys. **101**, 311 (1995).
[10] B. Villard and P.J. Nacher, Physica B **284**, 180 (2000).
[11] J. Jeener, Phys. Rev. Lett. **82**, 1772 (1999).
[12] E. Stoltz, J. Tannenhauser, and P.J. Nacher, J. Low Temp. Phys. **101**, 839 (1995).
[13] M.A. Bouchiat, T. R. Carver, and C. M. Varnum, Phys. Rev. Lett. **5**, 373 (1960).
[14] B.C. Grover, Phys. Rev. Lett. **40**, 391 (1978).
[15] T.G. Walker and W. Happer, Rev. Mod. Phys. **69**, 629 (1997).
[16] P.J. Nacher, G. Tastevin, B. Villard, N. Piegay, and K. Sauer, J. Low Temp. Phys. **121**, 743 (2000).
[17] Y.Y. Lin, N. Lisitza, S.D. Ahn, and W.S. Warren, Science **290**, 5489 (2000).